1

Conformal Window
and
Correlation Functions in Lattice Conformal QCD*

Y. Iwasaki

*University of Tsukuba,
Tsukuba, 305-8577, Japan*
*E-mail: iwasaki@ccs.tsukuba.ac.jp
www.ccs.tsukuba.ac.jp/people/iwasaki

We discuss various aspects of Conformal Field Theories on the Lattice. We mainly investigate the $SU(3)$ gauge theory with N_f degenerate fermions in the fundamental representation, employing the one-plaquette gauge action and the Wilson fermion action.

First we make a brief review of our previous works on the phase structure of lattice gauge theories in terms of the gauge coupling constant and the quark mass. We thereby clarify the reason why we conjecture that the conformal window is $7 \leq N_f \leq 16$.

Secondly, we introduce a new concept, "conformal theories with IR cutoff" and point out that any numerical simulation on a lattice is bounded by an IR cutoff Λ_{IR}. Then we make predictions that when N_f is within the conformal window, the propagator of a meson $G(t)$ behaves at large t, as $G(t) = c \exp(-m_H t)/t^\alpha$, that is, a modified Yukawa-type damping form, instead of the usual exponential damping form $\exp(-m_H t)$, in the small quark mass region where $m_H \leq c \Lambda_{IR}$ is satisfied: m_H is a generic mass of a hadron such as the pion mass and c is a constant of order 1. This holds on an any lattice for any coupling constant g, as far as g is between 0 and g^*, where g^* is the IR fixed point. We verify that numerical results really satisfy the predictions for the $N_f = 7$ case and the $N_f = 16$ case.

Thirdly, we discuss small number of flavors ($N_f = 2 \sim 6$) QCD at finite temperatures. We point out theoretically and verify numerically that the correlation functions at $T/T_c > 1$ exhibit the characteristics of the conformal function with IR cutoff, an exponential damping with power correction.

Investigating our numerical data by a new method which we call the "micro-analysis" of propagators, we observe that the $N_f = 7$ case and the $N_f = 2$ at $T \sim 2T_c$ case are similar to each other, while the $N_f = 16$ case and the $N_f = 2$ at $T = 10^2 \sim 10^5 Tc$ cases are similar to each other.

Further, we observe our data are consistent with the picture that the $N_f = 7$ case and the $N_f = 2$ at $T \sim 2T_c$ case are close to the meson unparticle model. On the other hand, the $N_f = 16$ case and the $N_f = 2$ at $T = 10^2 \sim 10^5 Tc$ cases are close to the fermion unparticle model. All results are consistent with naive physical intuition and solve long standing issues at high temperatures such as why the free energy at high temperatures does not reach the Stefan-Boltzmann ideal gas limit even at $T = 100 T_c$.

Keywords: Conformal Theories, Conformal Window, IR cutoff, Unparticle

2

1. Introduction and Summary

Recently there has been a lot of interest in finding a conformal or near-conformal theory, which could play a key role in constructing a theory Beyond the Standard Model (BSM) of particle physics.[1] Non-perturrbative investigation of non-supersymmetric conformal theories in four dimensional space-time is also ardently desired.

We already described in the abstract partly the objectives, the target, the method and the results of this work. In order to avoid to repeat the same things, we will skip what was described in the abstract and will describe remaining important matters.

The strategy we take is as follows: We define continuum conformal theories as the continuum limit of lattice theories. This is a constructive field theory approach. First, we propose the properties of continuum conformal theories from knowledge of the continuum super–symmetric conformal theories and RG argument.[2] Then, we conjecture the properties of lattice theories.

Lattice theories are defined on a Euclidian four-dimensional lattice with lattice size N_x, N_y, N_z, N_t and lattice spacing a. For simplicity, we assume $N_x = N_y = N_z = N$ and $N_t = rN$, with r a constant. The continuum limit of the theory is defined by $a \to 0$ with $N \to \infty$ keeping $L = N a$ constant. When L = finite, the continuum limit defines a theory with an IR cutoff.

We propose that the propagator of a meson $G(t)$ behaves at large t, as $G(t) = c \exp{(-m_H t)}/t^\alpha$ for a small enough quark mass. We note that this form of the propagator in the coordinate representation corresponds to a cut instead of a pole in the momentum representation.

After we have verified that numerical results satisfy the predictions for the $N_f = 7$ case and the $N_f = 16$ case, we propose a new method of analysis of propagators which we call the "micro-analysis of propagator": Writing the propagator of a meson as $G(t) = c \exp{(-m(t)t)}/t^{\alpha(t)}$, investigate the t dependence of $m(t)$ and $\alpha(t)$. The $m(t)$ and $\alpha(t)$ are reflected by the evolution of RG transformation flow and therefore contain useful information of the dynamics.

Carefully investigating the $m(t)$ and $\alpha(t)$, we observe that our data are consistent with the picture that the $N_f = 7$ theory is close to the meson unparticle model, while the $N_f = 16$ theory is close to the fermion unparticle model. We also observe the similarity between the large N_f case and the small N_f at $T \geq T_c$ case.

2. Stage and Tools

We employ the Wilson quark action and the standard one-plaquette gauge action. For fermion field an anti-periodic boundary condition is imposed in the time direction, otherwise periodic boundary conditions. The theory is defined by two parameters; the bare coupling constant g_0 and the bare quark mass m_0.

We usually use, instead of the bare gauge coupling constant g_0 and the bare quark mass m_0, β defined by $\beta = 6/g_0^2$ and $K = 1/2(m_0 a + 4)$, which is called the hopping parameter.

In order to investigate properties of the theory in the continuum limit, one has to first clarify the phase structure of lattice QCD at zero temperature to identify a UV fixed point and/or an IR fixed point. When $N_F \leq 16$, the point $g_0 = 0$ and $m_0 = 0$ is a UV fixed point. Therefore a theory governed by this fixed point is an asymptotically free theory. We restrict ourselves to the theory defined by this UV fixed point in this articles.

When there is an IR fixed point[3] at finite coupling constant g on the massless line which starts from the UV fixed point, the long distance behavior is determined by the IR fixed point. This defines a conformal theory. The minimum number of flavors N_f for the existence of such an IR fixed point is denoted by N_f^c. Usually $N_f^c \leq N_f \leq 16$ is called the conformal window.

The local meson operator is denoted by $G_H(t)$. When the theory is in the confining phase, it decays exponentially at large t

$$G_H(t) = c \exp(-m_H t) \tag{1}$$

for a free boundary, where m_H is the mass of the ground state hadron contained in the channel H.

The boundary conditions we take imply

$$G(t) = c \left(\exp(-m_H t) + \exp(-m_H (L_t - t)) \right) \tag{2}$$

for $t \to L_t/2$. From this behavior we extract the energy of the ground state m_H in the channel H.

The quark mass is defined through Ward-Takahashi identities

$$m_q = \frac{\langle 0|\nabla_4 A_4|\text{PS}\rangle}{2\langle 0|P|\text{PS}\rangle}, \tag{3}$$

where P is the pseudo-scalar density and A_4 the fourth component of the local axial vector current. Renormalization constants are suppressed, since this expression is enough for our purpose.

3. Phase Diagram: a brief survey of our previous works

In our earlier article,[4] we investigated the phase structure of the SU(3) and SU(2) gauge theory with various numbers of flavors N_f of Wilson fermions in the fundamental representation, and conjectured that the conformal window is $7 \leq N_F \leq 16$ for the SU(3) and $3 \leq N_F \leq 10$ for the SU(2), based on numerical results for various numbers of flavors.

Although we would like to extract the phase diagram at infinite volume and at zero temperature, we have to make simulations at finite volume N^3 and at finite $N_t = rN$. Therefore the phase diagram is a three dimensional space parameterized by, g_0, m_0 and N. Finally we have to take the limit N infinity.

4

3.1. $N_f \leq 6$

When N is finite, the phase diagram is given as in Fig. 1(a). In 1996, we studied[5] the finite temperature transition of QCD for $N_F =$2, 3, 6. Our results implies that the transition in the chiral limit is of first order for $N_f = 3$ and 6. The order of the chiral transition in the $N_f = 2$ case is more subtle. We will discuss this issue later.

At $K = 0$ which corresponds to the pure gauge theory, the phase transition is of first order. Thereby the transition line connects between the critical point at $K = 0$ and the chiral transition point at $K = K_c$.

As lattice size N increases, the phase transition points both at quenched QCD and at massless QCD move towards larger β as shown in Fig.1(b). Eventually in the limit $N \to \infty$, all the region is covered with the confinement phase as shown in Fig.3(a).

3.2. $7 \leq N_f \leq 16$

When N is finite, we found that the phase diagram is given as in Fig. 2(a). Due to the lack of chiral symmetry the structure of phase diagram is complicate.

The salient facts are the following:

First, the massless line which starts the UV fixed point moves towards smaller β and hits the bulk transition. The massless line belongs to a deconfining phase all through the region.

Secondly, in the confinement phase which exists at small β region there is no massless line. When we decrease the quark mass from the quenched QCD, we en-
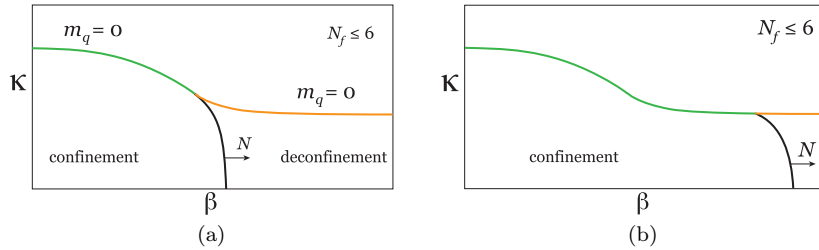

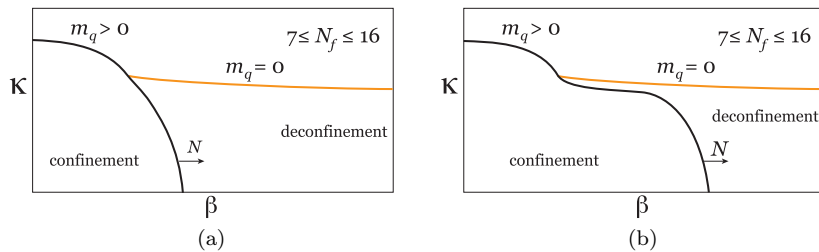Fig. 1.   Phase diagram for $N_f \leq 6$. (a) For not so large$N$. (b) For larger N.

Fig. 2.   Phase diagram for $7 \leq N_f \leq 16$. (a) For not so large$N$. (b) For larger N.

counter a bulk transition at finite quark mass. Thus this confinement phase is irrelevant to the continuum theory.

As lattice size N increases the phase diagram changes as shown in Fig.2(b) and Fig.3(b). It should be noted that there is still no massless line which belongs to a confinement phase. This implies that even in the continuum limit, the massless line does not belong to the confinement phase. On the other hand, if there would be no IR fixed point, the massless line should belong to a confining phase in the continuum limit. From this reasoning we conclude that the $N_f = 7$ theory is a conformal theory. Thus we conjecture that the conformal window is $7 \leq N_f \leq 16$.

4. Strategy for Identification of the Conformal Window

The logics in the previous work is an indirect way to identify the conformal window. Certainly more direct ways are desirable. The most direct and solid way is to identify the IR fixed point. However, for small N_f the IR fixed point exists deep in strong coupling region, and it becomes difficult to identify the IR fixed point.

An alternative way is to find directly the characteristics of conformal theories. This is the way we take in this work.

5. Conformal Field Theories

In this section we address ourselves to a basic and fundamental issue of what happens when the number of flavor N_f is within the conformal window.

The strategy we take is as follows: We define continuum conformal theories as the continuum limit of lattice theories. First, we propose the structure of continuum conformal theories from knowledge of the continuum super–symmetric conformal theories and RG argument. Then, we conjecture the structure of conformal theories on the lattice.

5.1. *Continuum Conformal Field Theories*

We discuss separately the $L = \infty$ case and the $L =$ finite case, since there exists a clear difference between the two cases.
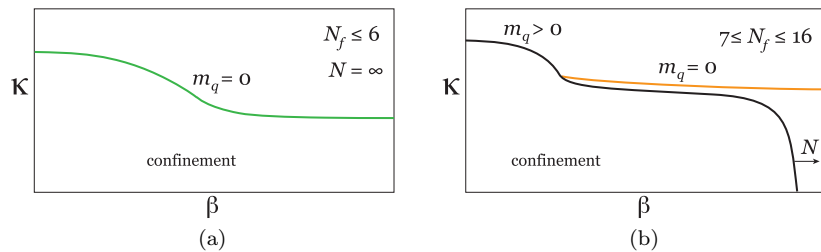

Fig. 3.   Phase diagra for large N. (a) For $N_f \leq 6$. (b) For $7 \leq N_f \leq 16$.

6

5.1.1. *The case $L = \infty$*

This defines a continuum theory on R^4 Euclidean four-dimensional space, which corresponds to the flat infinite space at zero temperature. In this case the IR cutoff Λ_{IR} is zero.

   Therefore the relevant quantity is only the running coupling constant $g(\mu)$ and there are no physical quantities which have physical dimensions.

   The "conformal region" exists only on the massless line. All other region is the "confinement region". The phase structure is shown in Fig.4(a). In super-symmetric theories this kind phase structure is known. The shaded region in the strong coupling region does not exist in the $\beta - m_q$ plane. When the phase structure is described in terms of $\beta - K$, the corresponding phase belongs to a region for Wilson doubles (Aoki phase). Therefore when it is mapped to the $\beta - m_q$ planes, the region corresponding to the shaded one does not exist.

   The propagator on the massless quark line takes the form

$$G(t) = c \frac{1}{t^\alpha}, \tag{4}$$

since, as mentioned, there is no physical quantities with physical dimensions.

   If we take the coupling constant $g = g^*$ at UV scale μ,

$$\alpha(t) = 3 - 2\gamma^*, \tag{5}$$

with γ^* being the anomalous mass dimension γ at $g = g^*$. The theory is scale invariant (and shown to be conformal invariant within perturbation theory.[6] See also e.g. Nakayama[7] and references therein from AdS/CFT approach). In general, the power α varies with t:

$$\alpha = \alpha(t). \tag{6}$$

   When t is small, the correlation function is governed by the UV fixed point. There the "meson" state is a free quark and an anti-quark state. Thus the power is given by

$$\alpha(t) = 3. \tag{7}$$

   When t is large, it is governed by the IR fixed point. The exponent is given by

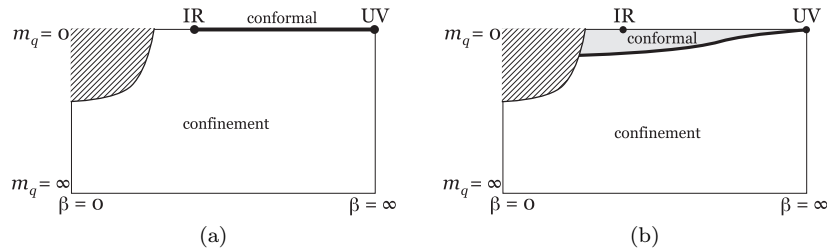$$\alpha(t) = 3 - 2\gamma^*. \tag{8}$$

Fig. 4.   Phase diagra for large $N = \infty$. (a) $\Lambda_{IR} = 0$. (b) $\Lambda_{IR} = $ finite

The exponent of the power α in IR is given by the renormalization equation or derived just by dimension counting.

5.1.2. *The case $L = $ finite*

This defines a continuum theory on T^4 Euclidean four-dimensional space, which corresponds to a compact T^3 space at finite temperature. In this case the IR cutoff $\Lambda_{IR} = 1/L$ is finite.

The renormalization transformation to IR does stop to evolve at the scale of IR cutoff Λ_{IR}. Thus the relevant physical quantities we may choose are

$$\Lambda_{CFT}, \Lambda_{IR}, m_H \tag{9}$$

Here Λ_{CFT} is a scale parameter for the transition region from UV to IR, and m_H is a generic mass of a meson such as the pion and the ρ meson.

Now we make a proposal. The propagator of a meson $G(t)$ behaves at large t, as

$$G(t) = c\frac{\exp(-mt)}{t^\alpha}, \tag{10}$$

that is, a modified Yukawa-type damping form in the region

$$m_H \leq c\,\Lambda_{IR}, \tag{11}$$

instead of the usual behavior of the propagator in the "confinement region",

$$G(t) = c\exp(-mt). \tag{12}$$

Here Λ_{IR} is an IR cutoff, m_H is a generic mass of a hadron such as the pion mass., and c is a constant of order 1. The "conformal region" is depicted in Fig.4(b). The relation eq.(11) reduces to

$$m_q \leq c\,(1/L)^{(1+\gamma^*)}, \tag{13}$$

using the relation[8]

$$m_H = c\,m_q^{1/(1+\gamma^*)}. \tag{14}$$

The phase structure with $L = $ finite smoothly approaches the case $L = \infty$, as L varies to ∞. The form of the propagator also smoothly becomes

$$G(t) = c\frac{1}{t^\alpha}, \tag{15}$$

in the massless limit.

As is the case in the $\Lambda_{IR} = 0$ case, the power α varies with t:

$$\alpha = \alpha(t). \tag{16}$$

When t is small,

$$\alpha(t) = 3. \tag{17}$$

8

On the other hand, when t is large ($t \gg 1/\Lambda_{CFT}$), the behavior of $\alpha(t)$ is complicate: When m is small enough and if $m\,t \ll 1$, the power is given by

$$\alpha(t) = 3 - 2\gamma^*. \tag{18}$$

If we take larger t such that $m\,t \gg 1$, the $\alpha(t)$ takes a value which depends on the dynamics of the theory. We give explicit examples when we discuss some models.

The concept of "conformal theory with IR cutoff" and "conformal region" determined by eqations (10) and (11) are our key proposals.

5.2. *Conformal Field Theories on the Lattice*

We are able to perform numerical simulations only on a finite size lattice. Thus the system is automatically bounded by the IR cutoff $\Lambda_{IR} \sim 1/(Na)$. In this case, the relevant physical parameters we may use are Λ_{CFT}, Λ_{IR} and m_H.

Our main target is first to verify the transition of a meson propagator from an exponential damping form to a modified Yukawa-type, that is, an exponential form with power correction given by eq. (10), at the critical hadron mass given by eq. (11).

When the lattice size N_1 increased to $N_2 = s\,N_1$ with β being fixed, then

$$m_H^{critical}(\beta, N_2) = 1/s\,m_H^{critical}(\beta, N_1). \tag{19}$$

The critical hadron mass decreases. Thus we have to carefully choose the simulation parameters in order to find the "conformal region" and the Yukawa-type propagators.

6. Numerical Simulations

6.1. *Algorithm and Parameters*

Table 1.   Parameters of Simulations

Nf	β	K	mq	Nf	β	K	mq	Nf	β	K	mq
7	6.0			16	11.5			2	6.5		
		0.1400	0.22			0.126	0.22			0.146	0.035
		0.1446	0.084			0.127	0.19		10.0		
		0.1452	0.062			0.130	0.10			0.135	0.028
		0.1459	0.045			0.1315	0.055		15.0		
		0.1472	0.006			0.13322	0.003			0.130	0.046

We have made simulations mainly for the cases $N_f = 7$ and $N_f = 16$, which are, we think, the boundaries of the conformal window. The algorithm we employ is the blocked HMC algorithm[9] for $N_f = 2\,N$ and the RHMC algorithm[10] for $N_f = 1$, in the case $N_f = 2\,N + 1$. The parameters we have simulated are listed in Table1. (The parameters for $N_f = 2$ at high temperatures are also listed.) We have chosen the hopping parameter K in such a way that the quark mass takes the value from

0.25 to 0.0. It might be worthwhile to mention that we are able to take K which corresponds to a negative quark mass crossing the zero quark mass, since the phase is a deconfining phase and therefore the pion mass is not zero there. The coupling constant of the IR fixed point for $N_f = 16$ is $\beta = 11.48$ in one-loop approximation. This is the reason why we choose $\beta = 11.5$ for $N_f = 16$.

The lattice sizes we choose are $8^3 \times 32, 16^3 \times 64$ and 24×96. The run-parameters are chosen such that the acceptance of the global metropolis test is about 70%. The statistics is in general 1,000 MD trajectories for thermalization and 1,000 MD trajectories for measurement.

7. Numerical Results

Let us first discuss the results for $N_f = 7$ case on a $16^3 \times 64$ lattice. Fig.5 shows the effective mass plots for pions with the local-sink local-source (black squares), local-sink doubly-smeared-source (red circles) and local-sink doubly-wall-source (green triangles) cases. The effective masses in the relatively large quark mass case shown on the left panel, $m_q = 0.25(K = 0.1400)$, clearly show the plateau at $t = 22 \sim 31$. On the other hand, in the $m_q = 0.045$ ($K = 0.1459$) case shown on the right panel, there is no plateau up to $t = 31$. The effective mass is slowly decreasing.

The effective masses for all cases with $m_q \leq 0.084$ ($K \geq 0.1446$) exhibit similar behavior to $K = 0.1459$. We have conjectured that propagators decay exponentially with power correction. Thus, to verify the conjecture, we fit the local-local data with the Yukawa-type for the fitting range $t = [15 : 31]$. The fits for $K = 0.1459$ and $K = 0.1452$ are depicted in Fig.6. The both fits well reproduce the data with range $t = [15 : 31]$ with $\alpha = 0.8(1)$.

In the case of $N_f = 16$, also, the effective masses on a $16^3 \times 64$ lattice exhibit the modified Yukawa-type for all cases when $K \geq 0.130$. The results of the fit to the local-local data for $K = 0.130$ and $K = 0.1315$ with the Yukawa-type for the fitting range $t = [15 : 31]$ are plotted in Fig.7. The fits well reproduce the data. However,
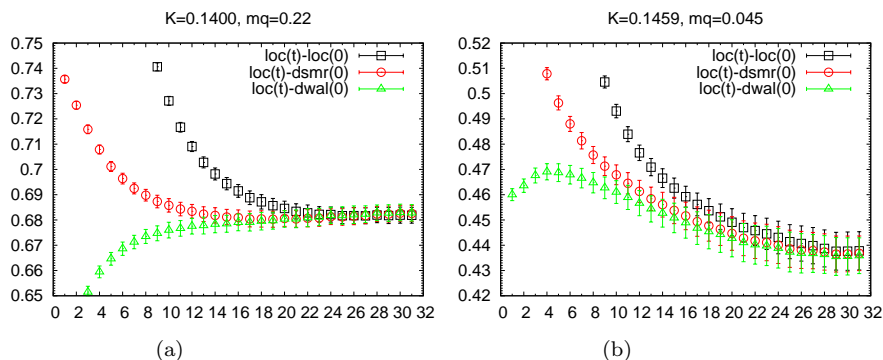

Fig. 5.   The asymptotic behavior of propagators in the $N_f = 7$ case on a $16^3 \times 64$ lattice at $\beta = 6.0$. (a) Exponential damping form.(b) Modified Yukawa-tye damping form.

10

if we carefully compare the fits of $N_f = 7$ and $N_f = 16$ cases, the fit of $N_f = 16$ case at large t is not so good as $N_f = 7$ case. We will discuss this point later.

The data on a $24^3 \times 96$ lattice for both cases of $N_f = 7$ with $K \geq 0.1459$ and $N_f = 16$ with $K \geq 0.130$ exhibit the modified Yukawa type decay.

Thus we have verified that the propagators decay with the Yukawa-type damping form for the $N_f = 7$ and $N_f = 16$ cases, for the small quark mass. In term of the pion mass the critical mass can be expressed as $m_H \leq c\,\Lambda_{IR}$. Here m_H is the pion mass and we take $\Lambda_{IR} = (N^3 \times N_t)^{1/4}$. There is no *a priori* definition of Λ_{IR} in the case of asymmetric lattices. This is one of choices. With this definition, we estimate the constant c is $c \sim 11.0$ for $N_f = 7$, and $c \sim 12.4$ for $N_f = 16$.
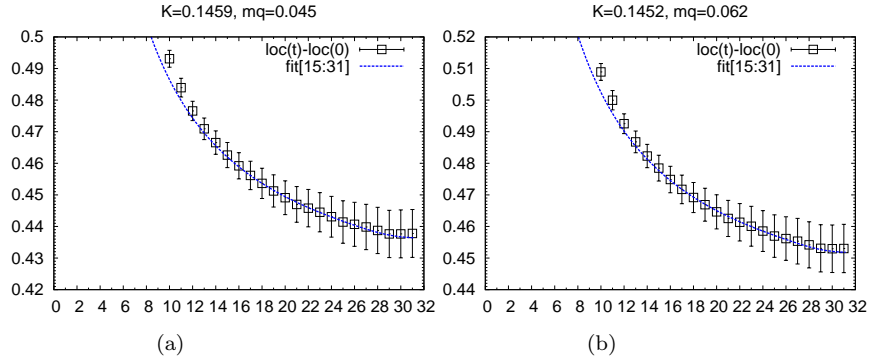
Fig. 6.   Two examples of modified Yukawa-type damping form in the $N_f = 7$ case on a $16^3 \times 64$ lattice at $\beta = 6.0$ (a) K=0.1459. (b) K=0.1452.
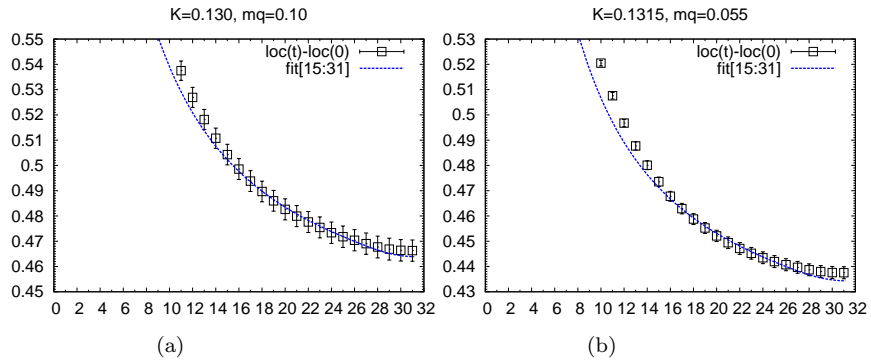

Fig. 7.   Two examples of modified Yukawa-type damping form in the $N_f = 16$ case on a $16^3 \times 64$ lattice at $\beta = 11.5$. (a) K=0.130. (b) K=0.1315.

8. Micro-analysis of Propagator

As we have verified our conjecture that the propagators decay with the Yukawa-type damping form for the small quark mass, the next issue we would like to solve is what kind of theory is defined. To do so, we propose a new method of analysis of propagators which we call the "micro-analysis" of propagators: Writing the propagator of a meson as

$$G(t) = c \exp\left(-m(t)t\right)/t^{\alpha(t)} \tag{20}$$

investigate the t dependence of $m(t)$ and $\alpha(t)$. The $m(t)$ and $\alpha(t)$ are reflected by the evolution of RG transformation flow and therefore contain useful information of the dynamics.

We depict $m(t)$ and $\alpha(t)$ in Figs.9∼ 19 for various cases.

First, at small t (we disregard the $\alpha(t)$ and $m(t)$ at $t = 1$ and 2, since they are affected by the boundary effect),

$$\alpha(t) \sim 3.0 \tag{21}$$

and

$$m(t) \sim 2\,m_q \tag{22}$$

are well satisfied, when $m_q \geq 1/N$.

As t increases, $m(t)$ increases from $2\,m_q$ to m_H. The behavior of $\alpha(t)$ is more complex and it reflects the dynamics.

In the $N_f = 7$ case on the $16^3 \times 64$ lattice, the $\alpha(t)$ at large t is relatively stable and it seems that $\alpha(t)$ shows a plateau at $t = 15 \sim 31$, although it is noisy. The statics of the data on the 24×96 lattice is not enough to see the $\alpha(t)$, as it requires more statistics than the Yukawa-type fit with a wider range of t. We are storing configurations.

The t dependence of $\alpha(t)$ in the $N_f = 16$ case is quite different from that of the $N_f = 7$ case. In the $N_f = 16$ case, although there is no plateau structure in $\alpha(t)$, there is a shoulder with a value around 1.5 at $t = 12 \sim 24$.on the $16^3 \times 64$ lattice. On the 24×96 lattice (the statistics is enough, since the $N_f = 16$ case is much faster than the $N_f = 7$ case), the t dependence of $\alpha(t)$ is different each other. In the case $K = 0.130$, the shoulder becomes very wide down to $t \sim 32$. In the case $K = 0.1315$ the shoulder is clearly seen for $t = 12 \sim 25$. on the other hand, the shoulder disappears and the plateau at $\alpha \sim 0.5$ is seen for $t \geq 24$ in the case $K = 0.13322$.

In order to find what kind of theory is defined, we will investigate some models which we consider are good candidates to compare with the theory. To do so, we find it is better to discuss conformal theories at high temperatures before that. Therefore we examine conformal theories at high temperatures in the next section.

12

9. Conformal Field Theories at Finite Temperature

Now let us consider lattice QCD at high temperatures for small N_f ($2 \leq N_f \leq 6$) where the chiral phase transition occurs at T_c. Note that the system is bounded by the infrared cutoff $\Lambda_{IR} = 1/T$. The continuum limit of the theory at finite temperature is defined by $a \to 0$ with $N \to \infty$ and $N_t \to \infty$ keeping $Na = L$ and $N_t a = 1/T$ constant. Taking the limit $L \to \infty$, the gauge theory at finite temperature T is defined.

We first consider the case that the renormalized quark mass is zero. Then the renormalized coupling constant is the only relevant variable in the theory. A running coupling constant $g(\mu; T)$ at temperature T can be defined as in the case of $T = 0$. The following discussion can be applied to any method of the definition of the running coupling constant $g(\mu; T)$. One way is the Wilson RG method.

Although in several literatures (see e.g. ref. 11) the running coupling constant $g(\mu; T)$ was discussed, it was mainly the UV behavior. Up to now it seems that it has not been discussed systematically the IR behavior.

In the UV region the running coupling constant at finite T is essentially as the same as that of $T = 0$. Since the theory is asymptotically free, at small g region the following relation

$$g^2(\mu; T) = g^2(\mu; T = 0) + cg^4(\mu; T = 0), \tag{23}$$

with c constant, is satisfied. The constant c depends on both of the schemes of $g(\mu; T = 0)$ and $g(\mu; T)$ in addition to N_f. It might be worthwhile to stress that the leading term is universal in the limit $g \to 0$.

However, in the IR region $g(\mu; T)$ may be quite different from $g(\mu; T = 0)$, since the IR cut-off Λ_{IR} in the time direction is $1/T$. This is quite different from the $T = 0$ case.

Furthermore, the fact that when $T/T_c > 1$, the quark is not confined, implies that the running coupling constant $g(\mu; T)$ cannot be arbitrarily large. This means that there is a fixed point in the β function when $T/T_c > 1$.

Let us increase the temperature gradually from $T = 0$.

As far as $T < T_c$, the β function is negative all through g. As the temperature is increased further, the form of β function will changes as in Fig.8: (a) When $T > T_c$
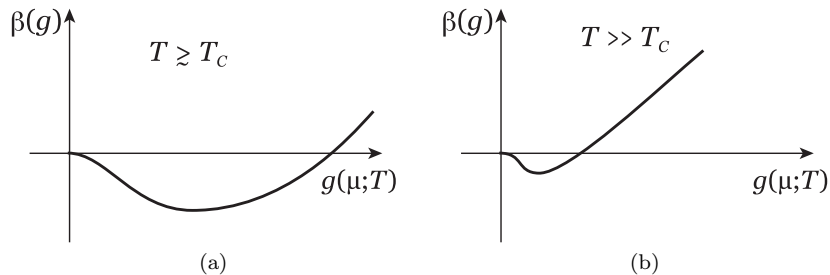

Fig. 8. β function with $T = $ constant. (a) $T \geq T_c$. (b) $T \gg T_c$.

but $T \sim T_c$, the β function changes the sign from negative to positive at large g.
(b) When $T \gg T_c$ it changes the sign at small g.

The T/T_c dependence of the β functions resembles the N_f dependence[3] for large N_f: $N_f = 16 \Leftrightarrow T/T_c \gg 1$ and $N_f = 7 \Leftrightarrow T/T_c \geq 1$.

9.1. *Numerical Results at HIgh Temperatures*

We have made simulation in the $N_f = 2$ case on a $16^3 \times 64$ lattice for several sets of parameters. Let us discuss the three cases listed in Table.1: $\beta = 6.5$ corresponds to $T \sim 2\,T_c$, $\beta = 10.0$ to $T \sim 100\,T_c$, and $\beta = 15.0$ to $T \sim 10^5\,T_c$.

We clearly see that the propagators in the three cases decay with the modified Yukawa type damping form. Therefore we make the "micro-analysis" of the propagators. The $m(t)$ and $\alpha(t)$ are depicted in Figs. 14, 15 and 16.

10. Correspondence between N_f and T

We observe the t dependence of $m(t)$ and $\alpha(t)$ in the case $T \sim 2T_c$ are very similar to those in the $N_f = 7$ case. On the other hand, the t dependence in the $T \sim 100T_c$ and $T \sim 10^5 T_c$ cases are very similar to those in the $N_f = 16$ case. We plot in Figs. 17, 18 and 19, the large N_f data on the right panel and the $N_f = 2$ at high temperature data on the left panel in order to compare them directly.

The similarities between them are excellent. We could anticipate this from the similarities of the β functions: $N_f = 16 \Leftrightarrow T/T_c \gg 1$ and $N_f = 7 \Leftrightarrow T/T_c \geq 1$.

We point out a possibility that there is a correspondence between the large N_f with Λ_{IR} and small N_f at high temperature T. Both of the large N_f with Λ_{IR} and the small N_f at high temperature T are described by two parameters in addition to N and N_t; β and m_q. In order to have a correspondence we have to map from one set of the parameters to the other set. Although It is too premature to discuss the details, the correspondence between N_f and T would be very intriguing and very useful. Although the flavor number N_f is a discrete integer, the temperature T is a continuous number. Thus the properties of large N_f could be deduced from those of small N_f at high temperatures with this correspondence.

11. Models

We investigate a few models to compare the results with the models.

(1) Meson unparticle model
(2) Fermion unparticle model
(3) A free quark and anti-quark state in the Wilson fermion formalism

The meson unparticle model and fermion unparticle model are motivated by the soft-wall model in AdS/CFT correspondence.[12]

(1) The soft-wall model predicts the form of the propagator with scale dimension

14

Δ in the momentum space as

$$\langle O(p)O(-p)\rangle = \frac{1}{(p^2 + m^2)^{2-\Delta}} \; . \tag{24}$$

In this case, when $m\,t \ll 1$, $\alpha(t) = 3 - 2\,\gamma^*$. This is model independent and universal. On the other hand, when $m\,t \gg 1$, $\alpha(t) = 2 - \gamma^*$ for $t \gg \Lambda_{CFT}^{-1}$. This is model dependent.

(2) Another plausible scenario is to treat $\bar{\psi}\gamma_5\psi(x)$ as the non-bound state of un-fermions. The soft-wall model predicts the form of the propagator with scale dimension Δ_f in the momentum space as

$$\langle \Psi(p)\bar{\Psi}(-p)\rangle = (p^\mu\gamma_\mu + m)\frac{1}{(p^2 + m^2)^{\frac{5}{2}-\Delta_f}} \; . \tag{25}$$

In this case, when $m\,t \ll 1$, $\alpha(t) = 3 - 2\,\gamma^*$. On the other hand, when $m\,t \gg 1$, $\alpha(t) = 1.5 - \gamma^*$ for $t \gg \Lambda_{CFT}^{-1}$. This is model dependent.

Let us discuss finite sizes effects. We have performed simulations at several lattice sizes up to $24^3 \times 96$. However $m_H = 0.2 \sim 0.4$ even for the massless quark $m_q \sim 0$ due to finite size effects. To obtain the γ^* from the scaling, eq.(5.1.2), finite size effects for m_H should be controlled. To estimate the finite size effects, we investigate them in the models.

- We make numerical investigation of finite size effects in the case of a free quark and an anti-quark state in the Wilson fermion formalism (with bare quark mass $m_0 = 0.20$). We make a Yukawa-type fit on N^4 lattices ($N = 24, 48, 64, 128, 160, 192$) using mathematica, and obtain for the exponent of the power and the mass of "meson".

$$\begin{aligned} p &= 1.5 + 95.8 \times N^{-5/4} \\ m_H &= 0.4 - 0.165 \times N^{-1/10} \; . \end{aligned} \tag{26}$$

To suppress the error of p to order 1%, we need $N \geq 50,000$. The finite size is much more severe than expected.

In the case of asymmetric lattice $N^3 \times 4N$, there is a shoulder taking the value $\alpha \sim 1.5$ at $N_t \sim N$, although the shape of the shoulder is not so clear as in the case $N_f = 16$.

- In the $N_f = 7$ case, finite size effects are expected to be similar to those of mesons in the confining phase: We need $N \geq 5 \times 1/m_H$.

- In the $N_f = 16$ case, severe effects are expected, since this case is similar to the free case.

12. What Kind of Theories are defined ?

First let us consider the $N_f = 16$ case. The t dependency of $\alpha(t)$ has a shoulder at $\alpha \sim 1.5$, except for the case $K = 0.13322$ on the $24^3 \times 96$ lattice. We also see a shoulder in the $N_f = 2$ case at $T \sim 100\,T_c$ and $T \sim 10^5\,T_c$ as well as in the free case. In the limit $T \to \infty$, the quark will become a free particle state ultimately.

Therefore we may consider that the state at very high temperatures in the $N_f = 2$ case is almost a free state, but is not. Then from the correspondence between N_f and T, which our data suggest, we conclude that our data are consistent with the picture that the $N_f = 16$ theory is close to the fermion unparticle model.

Next let us consider the $N_f = 7$ case. The t dependence of $\alpha(t)$ is very similar to the $N_f = 2$ case at $T \sim 2\,T_c$. We know that wave functions of meson just above T_c can be obtained numerically and a "meson" state is observed experimentally, although quarks are deconfined. This implies that the state just above T_c is a almost bound state, but it is not. Now, from the correspondence between N_f and T, we conclude that our data are consistent with the picture that the $N_f = 7$ theory is close to the meson unparticle model.

Now we estimate γ^* for $N_f = 7$ and $N_f = 16$, using the formula we have derived.

- We assume that the $N_f = 7$ case is well described by the meson unparticle model. The value of $\alpha(t)$ at plateau($t = 15 \sim 31$) is 0.8(1) for $K = 0.1452$ and $K = 0.1459$. Applying the formula $\alpha(t) = 2 - \gamma^*$, we have $2 - \gamma^* = 0.8(1)$. Thus $\gamma^* = 1.2(1)$. This is a crude estimate of γ^* based on some assumptions. The estimate should be much more refined.
- We assume that the $N_f = 16$ case is well described by the fermion unparticle model. With the value of $\alpha(t)$ at shoulder($t = 20 \sim 24$), $\alpha(t) \sim 1.5$, applying the formula $\alpha(t) = 1.5 - \gamma^*$, we have $1.5 - \gamma^* \sim 1.5$. From this we obtain $\gamma^* \sim 0.0$, which is consistent with a small value of 2-loop calculation; $\gamma^* \sim 0.025$.

13. Solutions for Long Standing Issues at High Temperatures

There are long standing issues at high temperatures.

(1) The free energy of quark-gluon plasma state does not reach that of the Stefan-Boltzmann ideal gas limit even at $T/T_c = 100$.[13]

(2) Wave functions of meson just above T_c can be obtained, although quarks are not confined.

(3) What is the order of the chiral phase transition in the $N_f = 2$ case, 1st or 2nd ? This is theoretically and phenomenologically important issue. Pisarski and Wilczek[14] derived that if the order parameter of chiral symmetry satisfies a scaling relation with exponents of the three dimensional $O(4)$ sigma model, the order is 2nd. We showed[15] that the scaling is well satisfied using the Wilson fermion formalism. Although it took some time, for staggered fermion, it was also shown that the scaling is satisfied in the $N_f = 2 + 1$ case.[16] Therefore it has been believed that this issue was settled down. However, recently, Sinya Aoki et al. have shown that under reasonable assumptions the effect of the $U_A(1)$ symmetry breaking does not contribute to some physical quantities.[17] This implies that the transition is 1st order. The issue has been revised.

Solutions for the issues are given as follows.

(1) When $T \gg T_c$, quarks are not free particles, but fermion unparticles. Therefore the degree of freedom will be effectively counted less than the free fermion case.

16

(2) When $T \sim T_c$, "mesons" are meson unparticles. Meson unparticles become mesons in the limit $T \to T_c$. Therefore meson unparticles are similar to meson particles in some aspects.

(3) In ref. 17, it is assumed that physical quantities are analytic in terms of m_q and m_H. However, $G(t)$ is not analytic in terms of m_q and m_H, as shown in this article. Therefore, the assumption of analyticity does not hold. Thus the conclusion that the chiral phase transition in the $N_f = 2$ case is 2nd order is revised.

14. Discussion and Conclusions

First of all, our conjectures for the conformal theories with IR cutoff have been verified in the cases of $N_f = 7$ and $N_f = 16$. This fact strengthens the assertion that the conformal window is $7 \leq N_f \leq 16$. We have further verified the Conformal Theories with IR cutoff in the case $T/T_c > 1$ for $N_f = 2$. We have stressed that IR cutoff is inherent with simulations on a lattice and QCD at high temperatures.

The "'micro-analysis" of propagators is proposed and is shown to be very useful. Even in the confining phase the t dependence of $\alpha(t)$ contains information of RG flow from UV to IR. If it is affected by an IR fixed point, it will appear as remnant in the $\alpha(t)$. If it is not affected, it is difficult to estimate γ^* correctly from the scaling rule, eq.(5.1.2).

By the "'micro-analysis" of the propagator, we observe "$N_f = 7$" and "$T \sim T_c$" are similar to each other, and "$N_f = 16$" and "$T \gg T_c$" are similar to each other. Using the correspondence between "N_f" and "T" that our data suggest, we conclude our data are consistent with the picture that "$N_f = 7$" and "$T \sim T_c$" are close to the meson unparticle model, and "$N_f = 16$" and "$T \gg T_c$" are close to the fermion unparticle model.

Surely a lot of things theoretically and numerically should be done. In particular, the continuum limit of propagators in the large N_f case should be estimated in order to obtain with more confident what kind of theories are defined. To do so, we have to investigate finite size effects and the β dependence of propagators. In parallel with these efforts, physics implications of unparticles such as the effects in the early universe should be much more deepened.

References

1. J. Giedt, PoS(Lattice 2012); E. Neil, PoS(Lattice 2011)009; L. Del Debbio, PoS(Lattice 2010)004; and references quoted.
2. K.G. Wilson and J. Kogut, Phys. Reports 12C (1974) 75.
3. T. Banks and A. Zaks, Nucl. Phys. **B196** (1982) 189.
4. Y. Iwasaki, K. Kanaya, S. Kaya, S. Sakai, and T. Yoshié, Phys. Rev. **D69** (2004) 014507.
5. Y. Iwasaki, K. Kanaya, S. Kaya, S. Sakai, and T. Yoshié, Phys. Rev. **D54** (1996) 7010.
6. J. Polchinski, Nucl. Phys. B **303**, 226 (1988).
7. Y. Nakayama, Int. J. Mod. Phys. A **25** (2010) 4849.
8. V.A. Miransky, Phys. Rev. **D59** (1999) 105003; L. Del Debbio and R. Zwicky, Phys. Rev. **D82** 014502.
9. M. Hayakawa, et al., PoS LATTICE **2010** (2010) 325.
10. M. A. Clark and A. D. Kennedy, Phys. Rev. Lett. **98** (2007) 051601.
11. O. Kaczmarek, F. Karsch, F. Zantow and P. Petreczky, Phys. Rev. **D70**(2004) 074505.
12. G. Cacciapaglia, G. Marandella and J. Terning, JHEP 0902, 049 (2009).
13. Sz. Borsanyi, et al., arXiv:1204.6184
14. R, Pisarski and F. Wilczek, Phys. Rev. **29** (1984) 338.
15. Y. Iwasaki, K. Kanaya, S. Kaya, and T. Yoshié, Phys. Rev. Lett. **78** (1997) 179.
16. S. Ejiri et al., Phys. Rev. **D80**(20049) 094505; A. Bazavov et al., Phys. Rev. **D85**(20012) 054503.
17. S. Aoki, H. Fukaya, Y. Taniguchi, arXiv:1209.2061
    .
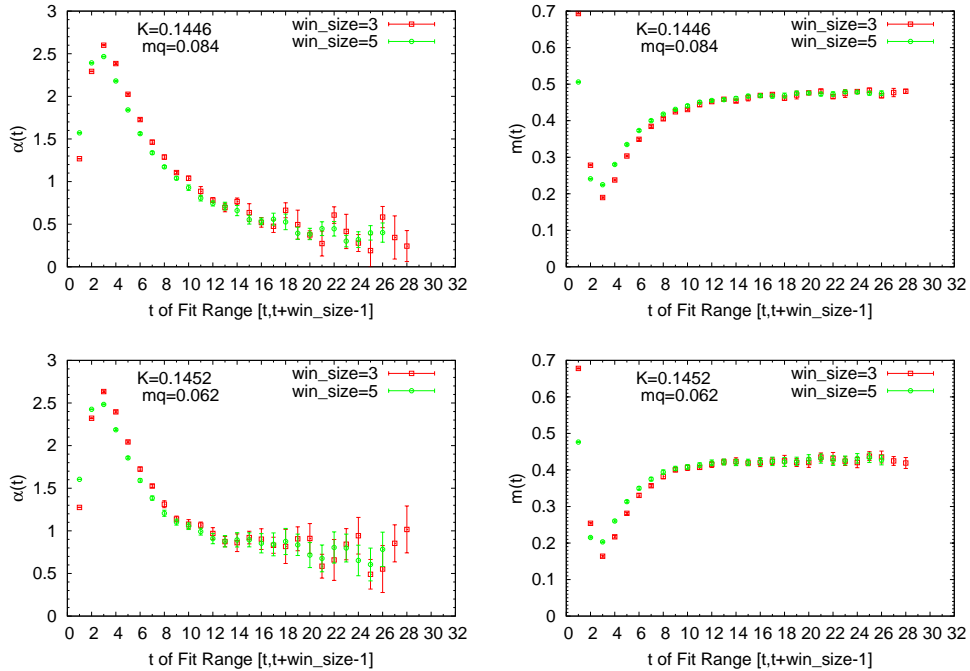
Fig. 9. $\alpha(t)$ and $m(t)$; $N_f = 7$ on a lattice $16^3 \times 64$ at $K = 0.1446$ and $K = 0.1452$

18
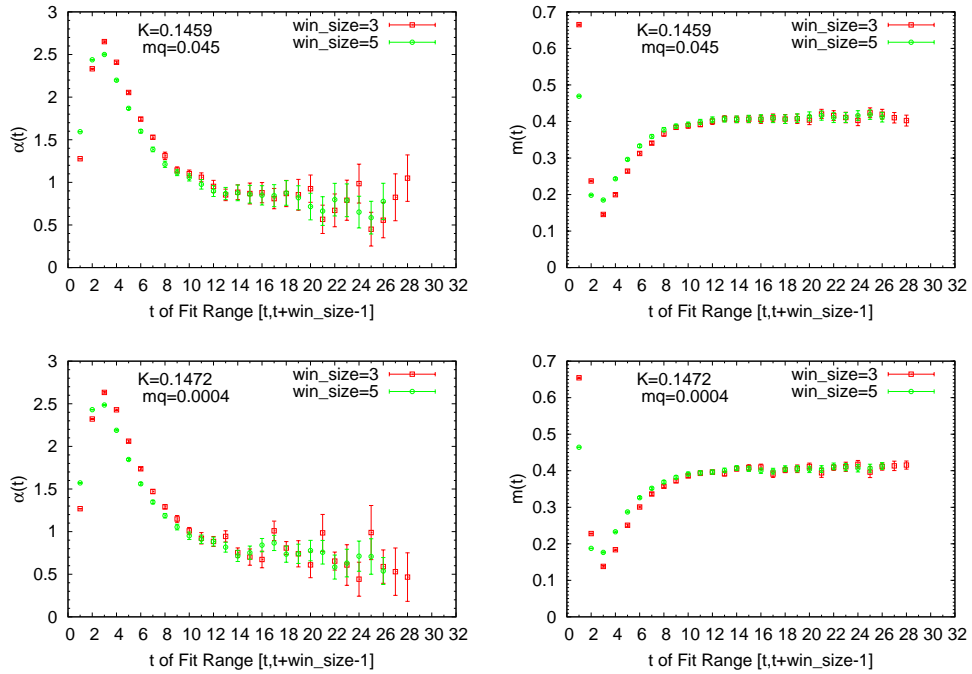
Fig. 10. $\alpha(t)$ and $m(t)$; $N_f = 7$ on a lattice $16^3 \times 64$ at $K = 0.1459$ and $K = 0.1472$
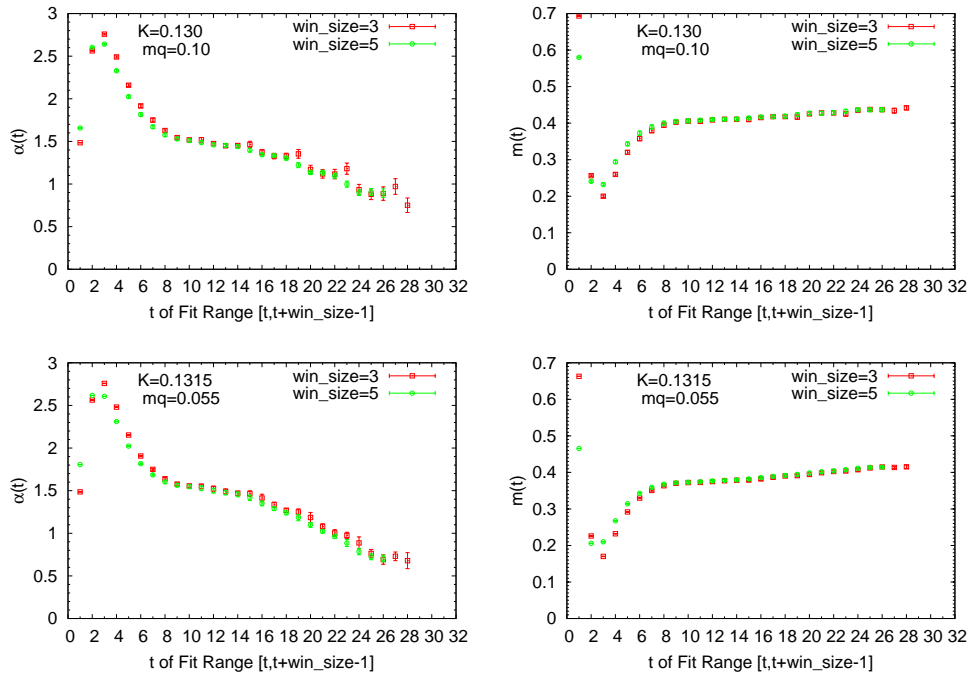

Fig. 11. $\alpha(t)$ and $m(t)$; $N_f = 16$ on a lattice $16^3 \times 64$ at $K = 0.130$ and $K = 0.1315$
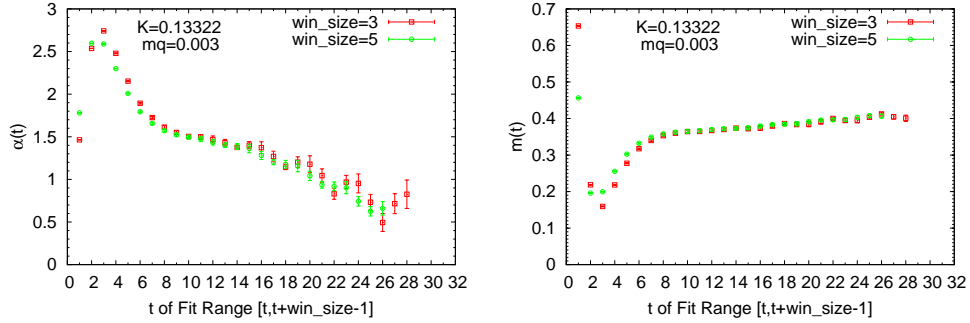
Fig. 12. $\alpha(t)$ and $m(t)$; $N_f = 16$ on a lattice $16^3 \times 64$ at $K = 0.13322$
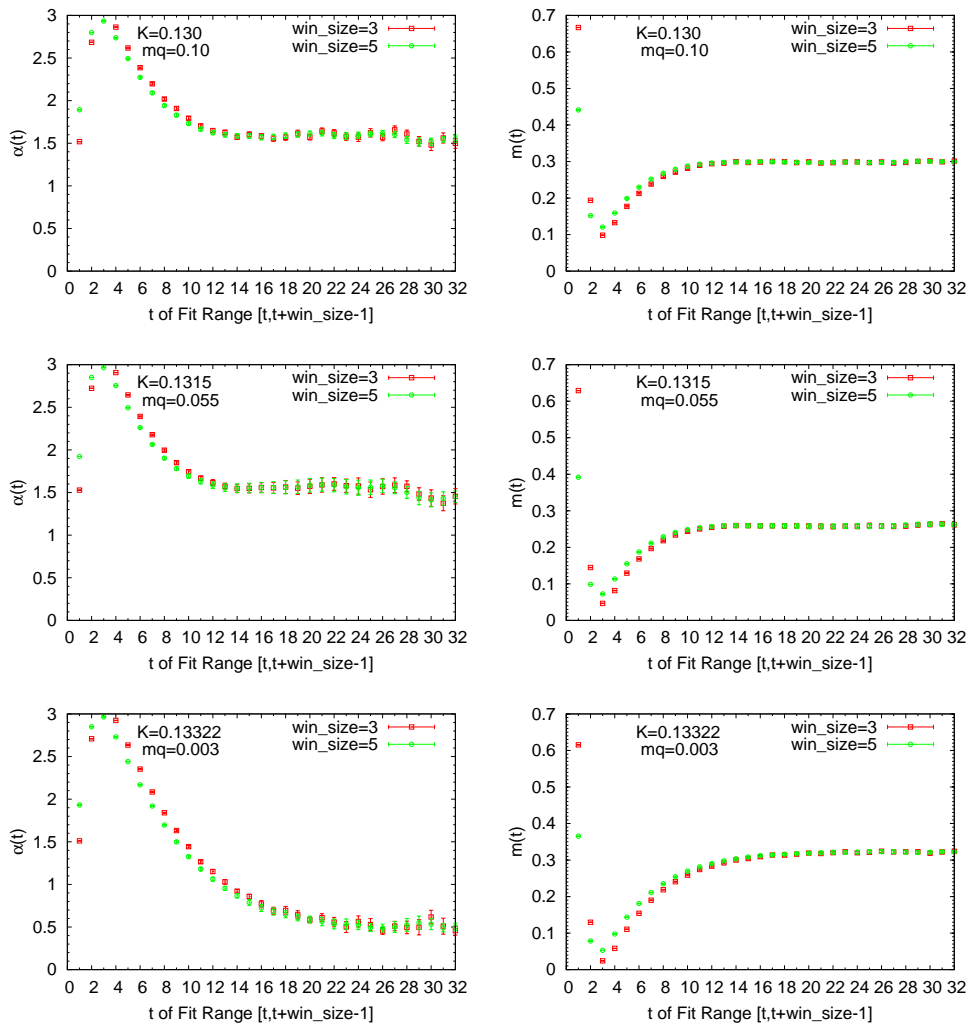

Fig. 13. $\alpha(t)$ and $m(t)$; $N_f = 16$ on a lattice $24^3 \times 96$ at $K = 0.130$, $K = 0.1315$ and $K = 0.13322$
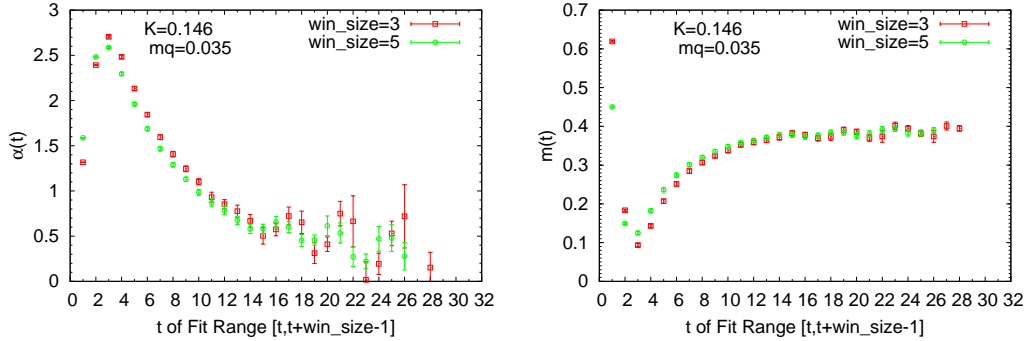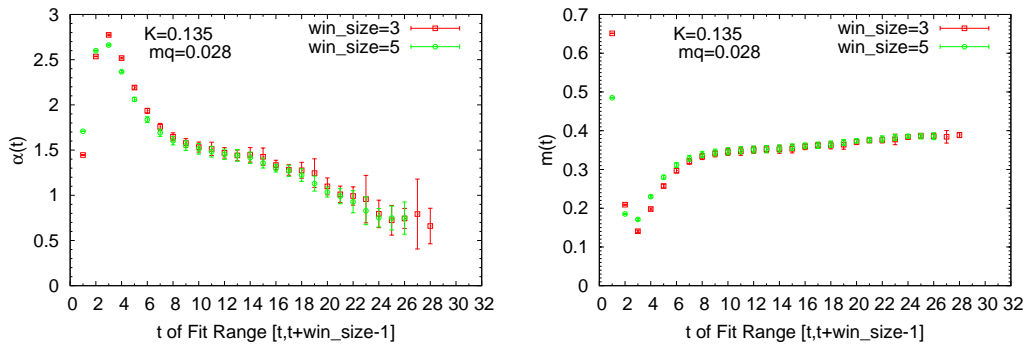
20

Fig. 14. $\alpha(t)$ and $m(t)$; $N_f = 2$ on a lattice $16^3 \times 64$ at $\beta = 6.5$ and $K = 0.146$.

Fig. 15. $\alpha(t)$ and $m(t)$; $N_f = 2$ on a lattice $16^3 \times 64$ at $\beta = 10.0$ and $K = 0.135$.
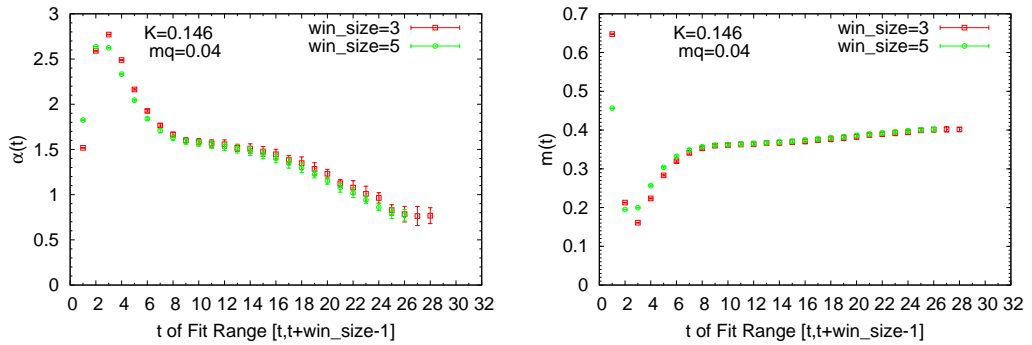

Fig. 16. $\alpha(t)$ and $m(t)$; $N_f = 2$ on a lattice $16^3 \times 64$ at $\beta = 15.0$ and $K = 0.130$.
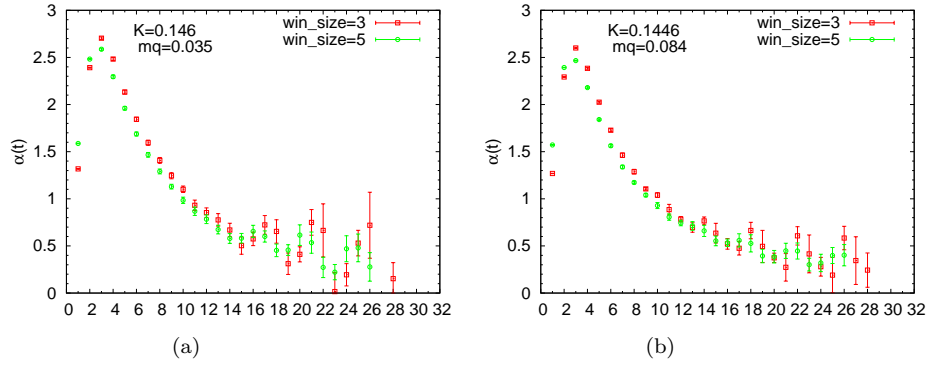
Fig. 17.   The exponent $\alpha(t)$ on a lattice $16^3 \times 64$.(a) $N_f = 2 T \sim 2\,T_c$.(b) $N_f = 7; K = 0.1446$.
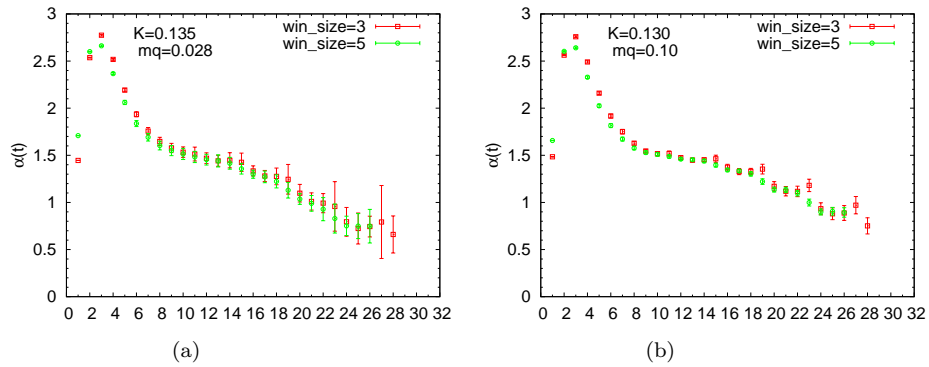

Fig. 18.   The exponent $\alpha(t)$ on a lattice $16^3 \times 64$. (a) $N_f = 2; T \sim 100\,T_c$. (b) $N_f = 16; K = 0.130$.
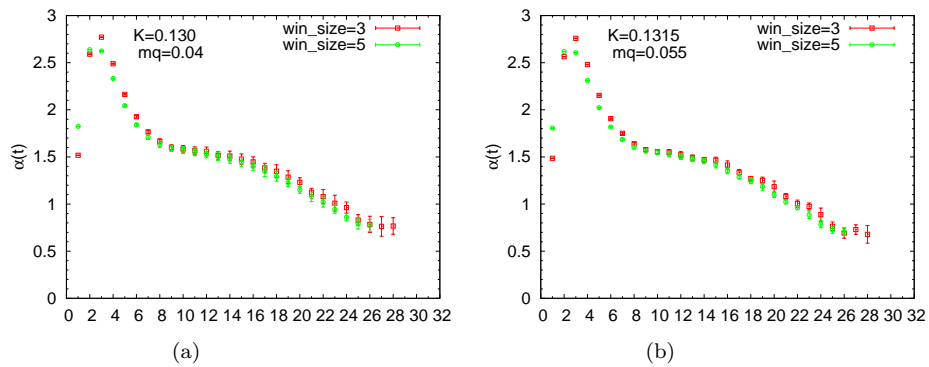

Fig. 19.   The exponent $\alpha(t)$ on a lattice $16^3 \times 64$. (a) $N_f = 2; T \sim 10^5\,T_c$. (b) $N_f = 16; K = 0.1315$.